

The Role of Colloidal and Particulate Fractions in REE Enrichments in Coal-Based Acid Mine Drainage Systems

Liliana Lefticariu^{1*}, Ryan L. Bowman¹, Madeline Lewinski¹,
Jerome Specht¹, and Paul T. Behum²

¹*School of Earth Systems and Sustainability, Southern Illinois University, Carbondale, 62901 USA*

²*Office of Surface Mining Reclamation and Enforcement, Alton, Alton, IL 62002 USA (retired)*

*Corresponding author lefticar@siu.edu, ORCID 0000-0003-3413-654X

Abstract

This work investigated the distribution, modes of occurrence, and relative extractability of rare earth elements (REE) from aqueous and solid waste at Tab Simco, an abandoned coal mining operation in Illinois, U.S.A. We found a preferential enrichment of REE-bearing phases in the aluminum-rich solid waste, which can contain up to 300 mg/kg of REE (corresponding to 0.04% REO), thus making it an attractive target for REE extraction. Additionally, existing technologies can sequester >90% of REE from AMD and concentrate them by a factor of 1000 in the solid precipitates. Coal-based waste could become a REE unconventional source.

Keywords: Rare earth elements, acid mine drainage, colloids, REE recovery stratification

Introduction

The rare earth elements (REE) are a group of 17 elements that include the lanthanides (Ln, atomic numbers 57 through 71), scandium (21), and yttrium (39) (IUPAC, 2005). The REE have similar atomic structure and geochemical behavior in natural systems and most are relatively abundant in the Earth's crust (McLennan, 2001). REE are essential in many industrial applications, including clean energy technologies, communications, and medical science (Kolker *et al.*, 2024). The REE global demand is predicted to increase up to seven times above the current levels by 2040 (U.S. DOE, 2023). Lately, the REE international market is challenged by continuously growing demand and limited supply, which could lead to shortages and engagements (Kolker *et al.*, 2024). Based on their economic prospect, Nd, Pr, Dy, and Tb are considered critical rare earths (i.e., *critical-REE*, U.S. DOE, 2023).

Coal mining waste (CMW), traditionally considered a byproduct of electric power generation, often contains REE and other critical materials (Kolker *et al.*, 2024). In CMW, REE are associated with REE-

bearing minerals (i.e., bastnäsite, monazite, xenotime, apatite, and zircon) or adsorbed onto clay minerals (Kolker *et al.*, 2024). In the Illinois coal basin, CMW at abandoned mining lands (AML) exhibited elevated REE contents ranging from 100 to over 300 mg/kg (Bowman, 2025). The REE concentration value of 300 mg/kg is considered the lower limit for economic profitability (U.S. DOE, 2023). Weathering of CMW materials, primarily those containing high amounts of pyrite (Lefticariu *et al.*, 2006), produces coal-based acid mine drainage (AMD), which is of environmental concern in coal basins worldwide. Although AMD is characterized by high acidity and elevated sulfate and iron contents, it may also contain economically relevant elements, including REE (Lefticariu *et al.*, 2020). It is uncertain what physical and biogeochemical processes exert primary control on the distribution of REE at AML sites.

In this contribution, we investigated the distribution, modes of occurrence, and relative extractability of REE from coal-based waste products, including AMD and CMW, at Tab Simco, an abandoned coal



mining operation in the Illinois Basin, U.S.A. (Behum *et al.*, 2011; Lefticariu *et al.*, 2020). We show that the preferential enrichments of REE-bearing phases occurs in the clay-rich particulate fraction, which can contain up to 300 mg/kg of total REE (corresponding to 0.04% REO), making it an attractive target for REE extraction. Existing technologies can sequester >90% of REE from AMD and concentrate them by a factor of 1000 in solid precipitates from which REE can be extracted using current technologies (Fujita *et al.*, 2024 and references therein). Together these data support the idea that coal-based waste materials at AML sites could become a promising secondary source of REE.

Methods

Multiple coal-based solid and aqueous samples were collected at different locations at Tab-Simco, an abandoned coal mining operation in the Illinois Basin, U.S.A. Details about sample locations are presented elsewhere (Lefticariu *et al.*, 2017; Bowman, 2025). The Tab Simco AML site is well suited for this study because it contains multiple AMD seeps and an AMD treatment system that includes a sulfate-reducing bioreactor and a wetland system designed to remediate AMD pollution (Behum *et al.*, 2011). Our team has studied the site and collected data for over fifteen years and the comprehensive breakdown of the methodology used for sample collection and analysis is available in our earlier work (Burns *et al.*, 2012; Lefticariu *et al.*, 2015; 2017; 2019; 2020;).

Briefly, the aqueous AMD samples were collected in 250-mL Nalgene™ HDPE bottles at various locations at the Tab Simco site following previously described procedures (Lefticariu *et al.*, 2017; Bowman, 2025). After collection, the samples were immediately transported on ice back to the SIUC Geochemistry Laboratory and filtered through 0.22 µm cellulose acetate membrane (Millipore® HAW). The filtered samples were analyzed for pH and conductivity by Mettler Toledo S400 Benchtop pH meter and dissolved sulfate by ion chromatography (IC). Cations analyses, including REE, were performed on filtered, acidified to pH < 2 using ultra-pure HNO₃ (Fisher

Scientific™) solution by Inductively Coupled Plasma Mass Spectroscopy (ICP-MS) at the ACME Laboratories, Inc. (Bureau Veritas Commodities), Vancouver, British Columbia, Canada. The solid samples derived from the weathering and passive treatment of CMW were collected across the Tab Simco AML site (Bowman, 2025). Additionally, multiple sediment cores were retrieved from the bioreactor representing mixtures of in situ precipitates and sediments generated by the weathering CMW and transported to the bioreactor (i.e., Lefticariu *et al.*, 2017; 2018). The retrieved samples were transported to SIUC, sectioned, dried at 50 °C, ground via mortar and pestle, and saved for further analyses. The metal, including REE, contents of solid matrix materials were determined by ICP-MS using a sodium peroxide fusion digestion method at Activation Laboratories, Inc. (Actlabs), Ancaster, Ontario, Canada. The mineralogical characterization was performed by powder X-ray diffraction (XRD) using a Rigaku Ultima IV X-ray diffractometer with CuKα radiation (Lefticariu *et al.*, 2017) and scanning electron microscopy with energy-dispersive X-ray spectroscopy (SEM-EDS) analyses using a Hitachi FlexSEM1000 SU1000 unit, with a Bruker EDS Unit attached for EDS analysis with a detection limit of 100 ppm (Bowman, 2025).

Results and Discussion

At the Tab Simco AML site, the weathering of CMW transferred its organic and inorganic constituents to the solution, which are transported as dissolved, colloidal, and/or particulate components by AMD and deposited across the site. Previous work showed that the primary dissolved (<0.22 µm) components in AMD were sulfate, SO₄, and ferrous iron, Fe(II), (Behum *et al.*, 2011) both sourced by pyrite oxidation (Lefticariu *et al.*, 2006). XRD analysis showed that the phyllosilicate minerals and quartz (Al-rich detrital phases, dNP) dominated the AMD colloidal and particulate fractions (Bowman, 2025). Additionally, the CMW-sourced aqueous Fe(II) was oxidized to ferric iron Fe(III), which through a series of microbially mediated processes that promoted the formation of Fe-rich phases

(i.e., schwertmannite, goethite), precipitated as neoformed nano- and micro-scale particles (nNP) (Lefticariu *et al.*, 2017). The field-scale bioreactor plays a key role in accumulating these dNP and nNP colloidal and particular fractions transported by AMD (Fig. 1a, b), such that over time, a thick sediment layer storing the accumulating dNP and nNP formed at the bottom of the pond above the bioreactor. Probing these AMD sediments allowed us to decipher the nature of the colloidal and particulate fractions as well as the biogeochemical processes that contributed to their formation and transformation (Lefticariu *et al.*, 2017)

The total concentration of REE (Σ REE) of various waste materials varies across the Tab Simco AML site (Bowman, 2025). The Σ REE of AMD samples from Tab Simco main seep ranged from 744.2 to 1000.2 $\mu\text{g/L}$ with an average of 898.3 $\mu\text{g/L}$ ($n = 8$) while *critical*- Σ REE (Nd, Pr, Dy, and Tb) varied between 192.5 and 258.1 $\mu\text{g/L}$ with an average of 224.9 $\mu\text{g/L}$. Overall, similar average Σ REE in AMD were noted from Tab Simco (Σ REE_{avg} = 898 $\mu\text{g/L}$) and Illinois basin AMD samples (Σ REE_{avg} = 1059 $\mu\text{g/L}$) (Lefticariu *et al.*, 2018).

The Σ REE contents of the AMD sediments at Tab Simco varied from 7 to 245 mg/kg (Bowman, 2025). Significantly, the concentrations of REE inversely correlate with Fe ($R^2 = 0.82$, $n = 18$) (Fig. 1c) and

directly correlate with Al ($R^2 = 0.91$, $n = 18$) (Fig. 1d), a trend consistently observed in AMD and CMW materials at AML sites throughout the Illinois Basin both (Lefticariu *et al.*, 2020; Bowman, 2025).

The normalized REE values to those of the Upper Continental Crust Reference (UCC; McLennan, 2001) further showed the large gap of the individual REE contents between the Al-rich and Fe-rich sediments (Fig. 1e). The Fe-rich sediments show an overall flat REE pattern, with value generally lower than 0.5, while Al-rich sediments exhibit more varied patterns displaying a Ce negative anomaly and enrichments in middle REE, namely Nd, Sm, Eu, and Gd (Fig. 1e). However, in terms of relative abundance of individual REE, similar patterns emerged for Fe-rich and Al-rich sediments, with the most abundant REE being Ce (33-36%), Ln (18-22%), Nd (14-16%), Y (11-13%), Pr (3-4%), Gd (2%), and Dy (2%). This surprising result suggests that contrary to the overall distinct mineralogy of the Al- and Fe-rich sediments, the REE may be hosted by similar phases. The *critical*- Σ REE (Nd, Pr, Dy, and Tb) contents varied between 1.7 and 7.7 mg/kg with an average of 4.8 mg/kg for Fe-rich sediments and between 27.2 and 48.7 mg/kg with an average of 40.2 mg/kg for Al-rich sediments. Overall, the Al-rich sediments contain one order of magnitude more REE than the

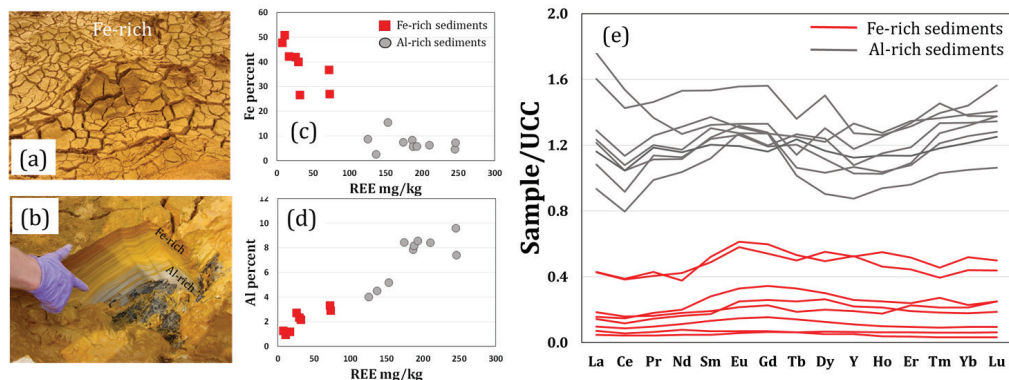


Figure 1 Composite picture depicting (a) and (b) close-up view of the Fe-rich and Al-rich sediments accumulated in the upper part of Tab Simco bioreactor (Lefticariu *et al.*, 2018); the dark material below the Al-rich sediment is the top of the organic compost layer (c) and (d) comparison REE values and Fe and Al, respectively of the AMD sediments; (e) REE patterns of Fe-rich and Al-rich sediments normalized to Upper Continental Crust Reference (UCC; McLennan, 2001).



Fe-rich sediments. In terms of the relative abundance of individual *critical*-REE, all AMD sediments exhibit similar patterns for Nd (69-74%), Pr (17-19%), Dy (8-10%), and Tb (1-2%).

The AMD sediments were further examined in detail by SEM and additional data were collected at the X-ray microprobe at Beamline 13-ID-E (GSECARS) at the Advanced Photon Source (APS), Argonne, IL (for details see Lefticariu *et al.*, 2017; 2018). The REE-bearing particulates were observable as trace phases by scanning electron microscopy and we measured the contents of REE in the particulates (Table 1; Bowman, 2025).

Our SEM analysis showed that the Fe-rich sediments contained no any discernible REE particles. Conversely, in the Al-rich AMD sediments, we were able to identify several REE-bearing particles, which were embedded within the clay-rich regions (Fig. 2a). These nano- and micro-scale REE-bearing particles were often embedded within the clay mineral assemblages (Fig. 2). The EDX-SEM measurements showed that REE-bearing particles exhibited elevated REE contents (Bowman, 2025), with values up to 5,535 ppm for La, 1845 ppm for Ce, and 73,994 for Nd (Table 1). Moreover, the high Al, Si, O, and low Fe contents suggest that the REE-bearing particles were embedded within the clays. Further mineralogical inves-

tigations revealed that phosphates, such as monazite ((Ce, Nd)PO₄), were the main (Ce,Nd)-bearing minerals in these sediments (Bowman, 2025).

Results of synchrotron X-ray analysis of the AMD sediments were previously reported (Lefticariu *et al.*, 2017; 2018). In terms of REE contents, we present here the Y spatial distribution in an Al-rich sediment sample as a Y-Ka μ XRF map (Fig. 2b). We used Y as a proxy for the REE since it has similar behaviour with the lanthanides (Kolker *et al.*, 2024). The map shows randomly distributed high-Y hot spots with sizes ranging from microns to nanometres (Fig. 2b). In the AMD sediments, Y was most probably incorporated into xenotime (YPO₄) and Y-bearing zircon (ZrSiO₄), which probably originated in the weathering CMW. Previously, we showed zircon, a ubiquitous accessory mineral in CMW, was present all AMD sediments as nano- and micro-scale particles. However, the particles' size and abundance were much higher in the Al-rich sediments (Lefticariu *et al.*, 2017).

The source of REE at the Tab Simco AMD system was the weathering CMW. Our recent investigation revealed that Σ REE of the CMW from the Illinois coal basin ranges from 100 to 310 mg/kg (Bowman, 2025). The common REE-bearing minerals in CMW include phosphates (i.e., monazite, rhabdophane, xenotime, apatite, and crandallite), silicates

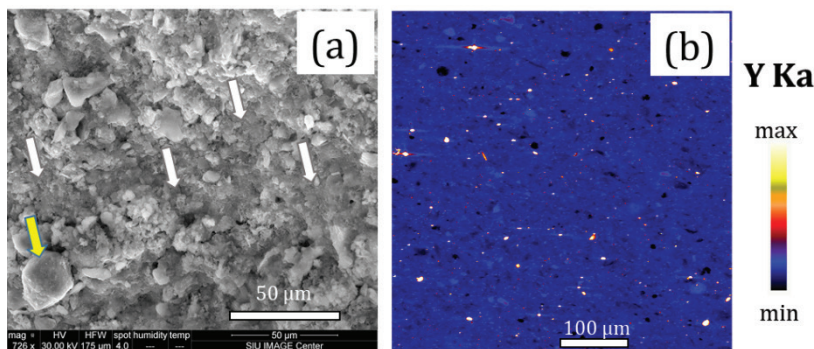


Figure 2 (a) SEM image of the sample from the Al-rich layer of the AMD sediments. The yellow arrow points to a quartz grain while the white arrows point to clay regions that host REE-bearing particulates. (b) Synchrotron X-ray fluorescence (XRF) elemental map of Yttrium (Y) in an Al-rich sediment sample (Lefticariu *et al.* in preparation).

Table 1 Chemical composition of REE-bearing particulate fraction in Al-rich samples from Tab Simco AML sites. Values in parts per million (ppm) (data from Bowman 2025).

Sample ID	C	O	Al	Si	Fe	La	Ce	Nd
Point #35	65675	537435	147574	229548	0	5535	1376	0
Point #38	105060	361644	153055	331257	0	303	675	0
Point #39	41071	270282	175780	348317	86085	2622	1845	73994
Point #40	84260	444743	107811	388262	23381	1529	12	0
Point #41	55340	416188	139550	331955	29963	787	82	26132
Point #42	55498	347804	155977	307194	62281	1221	1571	62140
Point #43	45515	529049	142525	223825	0	851	367	44953

(i.e., allanite, titanite, and zircon) and adsorption on clays (Kolker *et al.*, 2024). Physical and biogeochemical processes and mineral solubility controlled the weathering and partition of REE-bearing phases among various fractions. At Tab Simco, after the REE were released from their host minerals, they were transported as dissolved aqueous sulfate complexes and colloidal and particulate fractions. Highly acidic (pH <4) solutions, such as Tab Simco AMD (pH <3) are required to mobilize substantial amounts of REE due to the low solubility of REE-bearing minerals in neutral pH solutions. Phosphates usually weather rapidly in natural environments, releasing REE as either aqueous complexes or microscopic mineral particulates, which can adsorb onto clays and then be transported by AMD (Bowman, 2025).

In terms of CMW volume, the Fe-rich sediments are prevalent at Tab Simco (Leticariu *et al.*, 2017) and may represent an important sink for REE. However, recent work has demonstrated that REE adsorption onto Fe(III) precipitates is trivial at pH values lower than 5 (Lozano *et al.*, 2020). At Tab Simco, acidic waters characterized both the AMD, with pH <3, and the porewater of Fe-rich sediments, with pH <3.5, and therefore, the adsorbed REE fraction on Fe(III)-nNP is probably insignificant. Thus, Σ REE for Fe-rich sediments probably was the contribution of the detrital colloidal and particulate fraction. Clay minerals, particularly kaolinite and illite, can also sequester REE through weakly adsorption on their surfaces (Borst

et al., 2020). Clay-hosted REE deposits, a product of igneous rocks weathering in subtropical areas, are a major source of REE ores worldwide. As with Fe(III) sediments, the adsorption processes are controlled by pH, with clay's sequestration capacity for REE increasing at higher pHs (Bishop *et al.*, 2024). At Tab Simco, two factors could have controlled in the enhanced REE adsorption onto clays: the Al-rich sediments which contain high amounts of clays (i.e., kaolinite) and the pH values of their porewater were >5.5 (Leticariu *et al.*, 2017). In addition to REE adsorption on clays, the colloidal and particulate REE fraction markedly contributed to elevated Σ REE of the Al-rich sediments (Table 1). These processes resulted in the enhanced capacity of Al-rich sediments to sequester REE with Σ REE values ten times higher than those of Fe-rich sediments. Moreover, across the Illinois basin at the AML site, an accumulation of Al-rich sediments was observed, and in all cases, they contained higher REE contents (Bowman, 2025). Together, these results indicate that clay minerals could play an important role in the transport and sequestration of REE in AMD systems.

Conclusions

In this study, we show that in addition to the dissolved REE, there is a substantial fraction of REE carried as colloids and fine suspended particles that partition the REE between a truly dissolved fraction (<0.01 μ m) and the solid phases (>0.45 μ m). The preferential



enrichments of REE-bearing phases in the Al-rich sediments, which can contain up to 300 mg/kg of REE (corresponding to 0.04% REO) make it an attractive target for REE extraction. Additionally, existing technologies can sequester >90% of REE from AMD and concentrate them by a factor of 1000 in the solid precipitates (i.e., Fujita *et al.*, 2024 and references therein). Together these data strongly support the idea that Al-rich AMD sediments can become a promising secondary source of REE.

Acknowledgments

Synchrotron X-ray fluorescence (XRF) elemental maps were collected using the X-ray microprobe at Beamline 13-ID-E (GSECARS) at the Advanced Photon Source (APS), Argonne, IL. This research was supported by grants from the Department of Energy (DE-FE0032049) and NASA (80NSSC21K180).

References

- Behum PT, Lefiticariu L, Bender KS, Segid YT, Burns AS, Pugh CW (2011) Remediation of coal-mine drainage by a sulfate-reducing bioreactor: A case study from the Illinois coal basin, USA. *Appl. Geochem.* 26: S162-S166.
- Bishop BA, Alam MS, Flynn SL, Chen N, Hao W, Ramachandran SK, Swaren, L., Gutierrez RD., Konhauser KO, Alessi DS, Robbins LJ (2024). Rare Earth Element adsorption to clay minerals: mechanistic insights and implications for recovery from secondary sources. *Environ. Sci. Technol.* 58(16):7217-7227.
- Borst AM, Smith MP, Finch AA, Estrade G, Villanova-de-Benavent C, Nason P, Marquis E, Horsburgh NJ, Goodenough KM, Xu C, Kynický J (2020) Adsorption of rare earth elements in regolith-hosted clay deposits. *Nat. Commun.* 11(1):4386.
- Bowman RL (2025) Illinois abandoned mine lands: possibilities for sourcing critical minerals in coal mining waste. Ph.D. thesis, Southern Illinois University, Carbondale, Illinois.
- Burns AS, Pugh CW, Segid YT, Behum PT, Lefiticariu L, Bender KS (2012) Performance and microbial community dynamics of a sulfate-reducing bioreactor treating coal generated acid mine drainage. *Biodegradation* 23:415-429.
- Fujita Y, Park D, Lencka M, Anderko A, Reed D, Thompson V, Das G, Eslamimanesh A, Jiao Y (2024) Beneficiation of Rare Earth Elements: Prospects for Biotechnology Deployment. In *Rare Earth Elements: Sustainable Recovery, Processing, and Purification* (pp.251-297). American Geophysical Union: Willey Publishing.
- IUPAC (2005) In: Connelly, N.G. Hartshorn, R.M. Damhus, T. Hutton A.T. (Eds.) *Nomenclature of Inorganic Chemistry-IUPAC Recommendations*.
- Kolker A, Lefiticariu L, Anderson ST (2024) Energy-Related Rare Earth Element Sources. In *Rare Earth Metals and Minerals Industries: Status and Prospects* (pp. 57-102). Cham: Springer International Publishing.
- Lefiticariu L, Klitzing KL, Kolker A (2020) Rare Earth Elements and Yttrium (REY) in coal mine drainage from the Illinois Basin, USA. *Int. J. Coal Geol.* 217:103327.
- Lefiticariu L, Pratt LM, Ripley EM (2006) Mineralogical and sulfur isotopic effects accompanying oxidation of pyrite in millimolar solutions of hydrogen peroxide at temperatures from 4 to 150 C. *Geochim. Cosmochim. Acta* 70(19):4889-4905.
- Lefiticariu L, Sutton SR, Bender KS, Lefiticariu M, Pentrak M, Stucki JW (2017) Impacts of detrital nano- and micro-scale particles (dNP) on contaminant dynamics in a coal mine AMD treatment system. *Sci Total Environ.* 575:941-955.
- Lefiticariu L, Sutton SR, Lanzirrotti A, Flynn TM (2019) Enhanced immobilization of arsenic from acid mine drainage by detrital clay minerals. *ACS Earth Space Chem.* 3(11):2525-2538.
- Lefiticariu L, Walters ER, Pugh CW, Bender KS (2015) Sulfate reducing bioreactor dependence on organic substrates for remediation of coal-generated acid mine drainage: Field experiments. *Appl. Geochem.* 63:70-82.
- Lozano A, Ayora C, Fernández-Martínez A (2020) Sorption of rare earth elements on schwertmannite and their mobility in acid mine drainage treatments. *Appl. Geochem.* 113:104499.
- McLennan SM (2001) Relationships between the trace element composition of sedimentary rocks and upper continental crust. *Geochem. Geophys. Geosyst.* 2(4), doi:10.1029/2000GC000109
- U.S. Department of Energy, DOE (2023) Critical Materials Assessment, https://www.energy.gov/sites/default/files/2023-07/doe-critical-material-assessment_07312023.pdf